Supporting Information for On-Surface Carbon Nitride Growth from Polymerization of 2,5,8-Triazido-*s*-heptazine

Matthias Krinninger,[†,‡,¶] Nicolas Bock,[†,‡] Sebastian Kaiser,[†,‡] Johanna Reich,[¶,‡] Tobias Bruhm,[§,‡] Felix Haag,[‖] Francesco Allegretti,[‖] Ueli Heiz,[†,‡] Klaus Köhler,[§,‡] Barbara A.J. Lechner,[¶,‡,⊥] and Friedrich Esch[*,†,‡]

†*Technical University of Munich, TUM School of Natural Sciences, Department of Chemistry, Chair of Physical Chemistry, Lichtenbergstr. 4,D-85748 Garching, Germany*

‡*Catalysis Research Center, Technical University of Munich, Ernst-Otto-Fischer-Str. 1, D-85748 Garching, Germany*

¶*Technical University of Munich, TUM School of Natural Sciences, Department of Chemistry, Functional Nanomaterials Group, Lichtenbergstr. 4, D-85748 Garching, Germany*

§*Technical University of Munich, TUM School of Natural Sciences, Department of Chemistry, Professorship of Inorganic Chemistry, Lichtenbergstr. 4, D-85748 Garching, Germany*

‖*Technical University of Munich, TUM School of Natural Sciences, Department of Physics, Chair of Experimental Physics (E20), James-Franck Str. 1, D-85748 Garching, Germany*

⊥*Institute for Advanced Study, Technical University of Munich, Lichtenbergstr. 2a, D-85748 Garching, Germany*

E-mail: friedrich.esch@tum.de

S1. Polymerization reaction

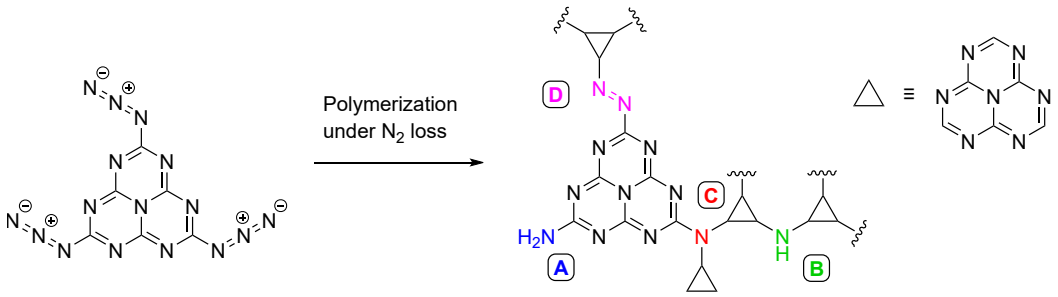

Figure S1: Reaction scheme showing the suggested pathway from 2,5,8-triazido-s-heptazine (TAH) to the 2D polyheptazine-based network. The azide groups decompose under nitrogen loss, forming nitrene intermediates. Their coupling, assuming that the π-bonded core remains intact, is discussed in the literature to proceed to the indicated products: terminal primary amines (A), linking via secondary amines - leading to poly(heptazine imides) - (B), 2D linking via tertiary amines (C) or via azo groups (D). Tertiary amines, found in the polymerization of TAH powders, might be formed by the sequential nitrene attack of azo-coupled nitrogens, under N_2 loss.

S2. TAH synthesis and characterization of purity

The synthesis of 2,5,8-triazido-*s*-heptazine (TAH) followed the reports of Sattler et al.[1] and Saplinova et al.[2] In a first step, melamine was heated to 663 K in a porcelain crucible, covered with a lid, in a muffle furnace for 24 hours. In order to remove undesired side products, the raw product was then heated under reflux in acetic acid for 3 hours to get the *s*-heptazine based melem (2,5,8-triamino-*s*-heptazine).

In the next step, the amino groups of melem were converted into hydrazine groups. To that purpose, the suspension of melem in hydrazine monohydrate was heated to 413 K for 24 hours in a glass lined stainless steel autoclave. The reaction mixture was purified by repetitive dissolution in hydrochloric acid, filtration and precipitation by addition of sodium hydroxide solution. The thus obtained product, 2,5,8-trihydrazino-*s*-heptazine was suspended in hydrochloric acid and dropped into a 278 K cold solution of $NaNO_2$ in hydrochloric acid. After stirring for 3 hours, the solid was filtered off, washed with water and ethanol to yield the final product TAH.

To characterize the purity of the obtained TAH precursor, we performed ^{13}C-NMR, ATR-FTIR and Raman spectroscopy (see Fig. S2), as well as elemental analysis, and compared to the characterization by Miller.[3,4] While both ^{13}C-NMR spectra show only two carbon signals, as expected for a pure precursor, our elemental analysis contains much less residual hydrogen (0.13 wt% as compared to 0.88 wt% in ref.[3]).

The ATR-FTIR spectrum of TAH in Fig. S2a shows the characteristic peak at 817 cm^{-1}, representative for triazine and heptazine ring breathing modes, a bunch of vibrational C−N and C=N modes in the $1200 - 1700$ cm^{-1} region and the characteristic azide modes at $2144 - 2229$ cm^{-1}, while N−H stretching mode in the range between 3300 and 3500 cm^{-1} are missing. Most of these peaks are also found in the Raman spectrum of the TAH precursor in Fig. S2b.

When reacting the powder at the indicated temperatures in vacuum or in argon (upper spectra in Fig. S2a), one observes the disappearance of the azide peaks, while the heptazine

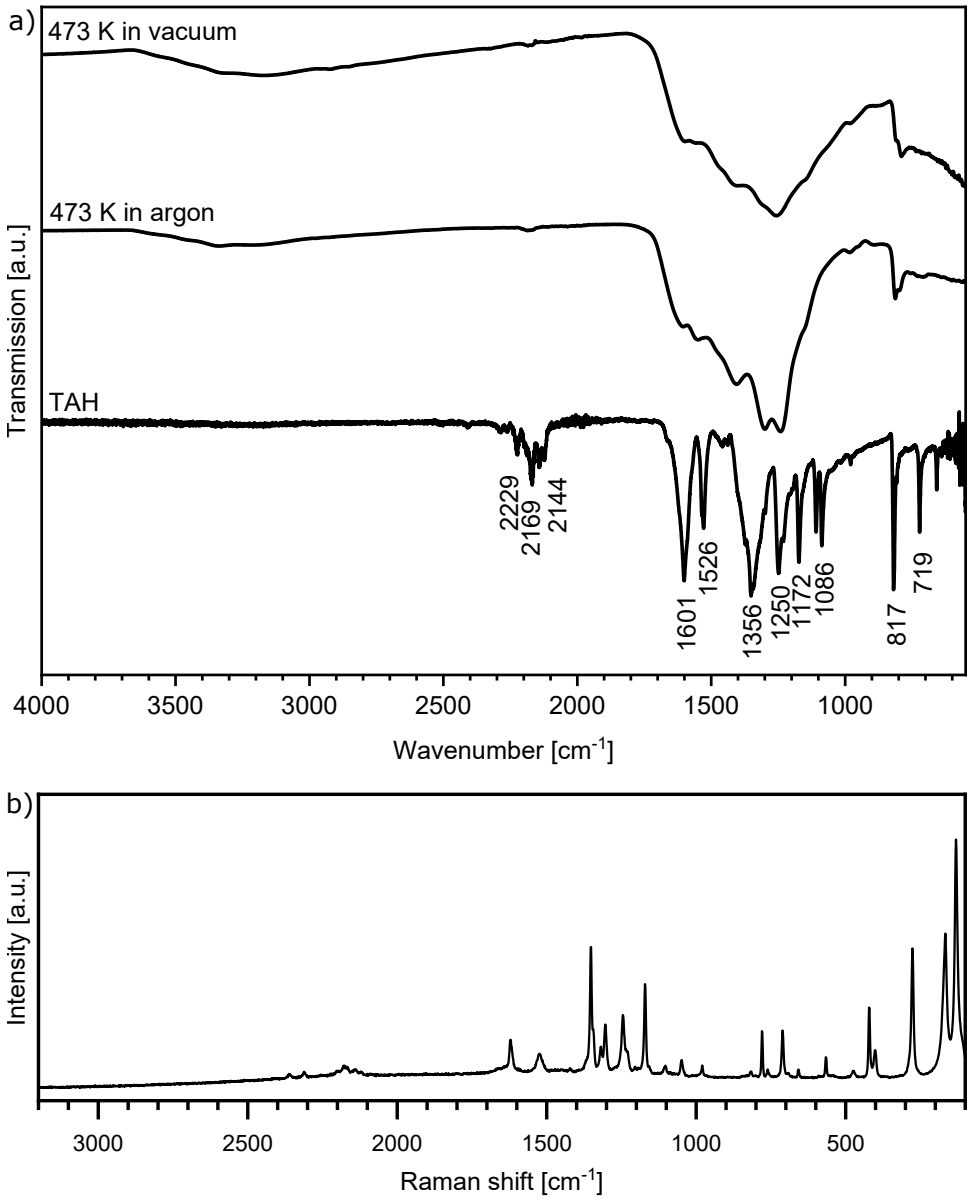

Figure S2: Characterization of the TAH precursor powder and its annealing products by vibrational spectroscopy: (a) ATR-FTIR spectra of TAH (bottom spectrum) and reaction products after heating to 473 K under argon (center) or in vacuum conditions (top spectrum). The TAH molecule can be identified by the s-heptazine, triazine and azide vibrations (see text and detailed list below). The azide contribution at $2144 - 2229$ cm^{-1} disappears for the reacted carbon nitride, while N−H species form. (b) Raman spectrum of TAH.

ring breathing mode at 817 cm^{-1} persists, although as a broader feature, indicating that the conjugated ring structure remains intact. In the azide peak region, a small peak at 2190 cm^{-1} remains that Miller et al. assign to the possible formation of imine side products (=C=NH, nitrile −C≡N, or diimide −N=C=N−.[4]

^{13}C-NMR (101 MHz, DMSO-d6) δ(ppm) = 158.8 (s, N=C−N), 171.5 (s, C−N_3).

Elemental analysis (wt%): Calc. C (24.33), N (75.67); Found C (24.15), N (73.64), H (0.13).

FTIR (ATR, 25 °C, cm^{-1}): 2406 (w), 2284 (w), 2229 (w), 2169 (m), 2144 (w), 2118 (w), 1601 (s), 1526 (m), 1356 (s), 1250 (s), 1172 (s), 1106 (s), 1086 (s), 977 (w), 817 (s), 719 (s), 657 (m).

Raman (785 nm, 25 °C, cm^{-1}): 2361 (w), 2310 (w), 2176 (w), 2141 (w), 2121 (w), 1621 (w), 1522 (w), 1353 (s), 1318 (w), 1304 (m), 1246 (m), 1170 (m), 1102 (w), 1050 (w), 978 (w), 815 (w), 776 (m), 757 (w), 711 (m), 660 (w), 566 (w), 476 (w), 422 (m), 401 (w), 280 (s), 168 (s), 130 (s).

S3. TAH evaporation process

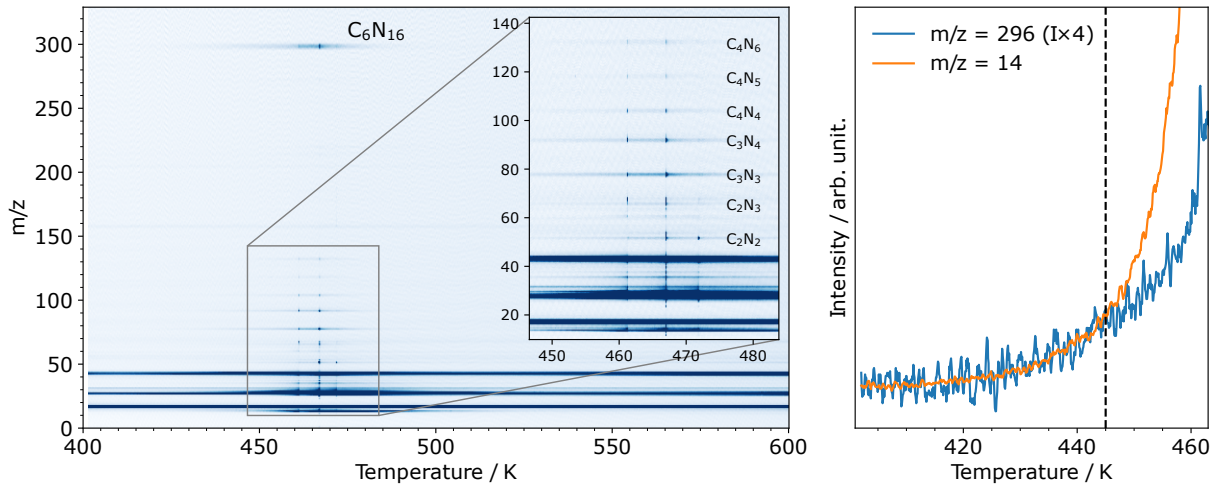

Figure S3: Thermal desorption of TAH powder from a crucible mounted in front of a quadrupole mass spectrometer. The mass spectra were measured from $m/z = 1$ to 600, by heating in high vacuum (p_{bg}<5×10^{-8} mbar) with a temperature ramp of 0.05 K/s.
(left) The overview scan that displays mass traces up to $m/z = 300$ clearly indicates a distinct peak of intact TAH (C_6N_{16}, $m/z = 296$), detected around 470 K, as well as several fragment signals in the range between $m/z = 52$ and $m/z = 132$, most likely originating from fragmentation in the QMS. We assign the fragment $m/z = 78$ to *s*-triazine (C_3N_3), which has a comparatively strong intensity thanks to its conjugated π-system. Further signals are present throughout the entire temperature range and arise from residual gases in the vacuum chamber, i.e. H_2O ($m/z = 18$), CO ($m/z = 28$) and CO_2 ($m/z = 44$). Distinct spikes in the fragment signals around the TAH desorption maximum hint at possible molecule ejection caused by autocatalytic microexplosions at slightly hotter spots inside the crucible-located powder. No polymerization products with $m/z > 300$ are detected.
(right) The signal $m/z = 14$ relates to nitrogen that stems from two processes: The decomposition of TAH in the crucible and the fragmentation of evaporated TAH in the QMS. We discriminate the two by overlaying the TAH signal ($m/z = 296$) onto the initial $m/z = 14$ rise. TAH decomposition in the powder and hence polymerization thus sets in at the temperature where the nitrogen curve starts to deviate from the TAH curve (indicated by a vertical dashed line). We therefore deduce the ideal evaporation temperature range to be just below 445 K.

S4. Reference measurements on HOPG

As illustrated in the thermal desorption spectra in Fig. 3a, the interaction of TAH with an HOPG support is substantially weaker than within the powder: TAH is not bound sufficiently strongly to activate the thermal decomposition before desorption. TAH on HOPG can, however, be activated by X-ray illumination. While TAH decomposes almost immediately on Au(111), making it impossible to trace the azide functionality in the N 1s XPS spectra, the activation on HOPG is less immediate. This difference in reactivity points to the involvement of secondary electrons in X-ray activation. It allows to prove intact azide adsorption on the HOPG support and its subsequent decomposition (Fig. S4) and to image the network that forms upon polymerization and subsequent annealing (Fig. S5).

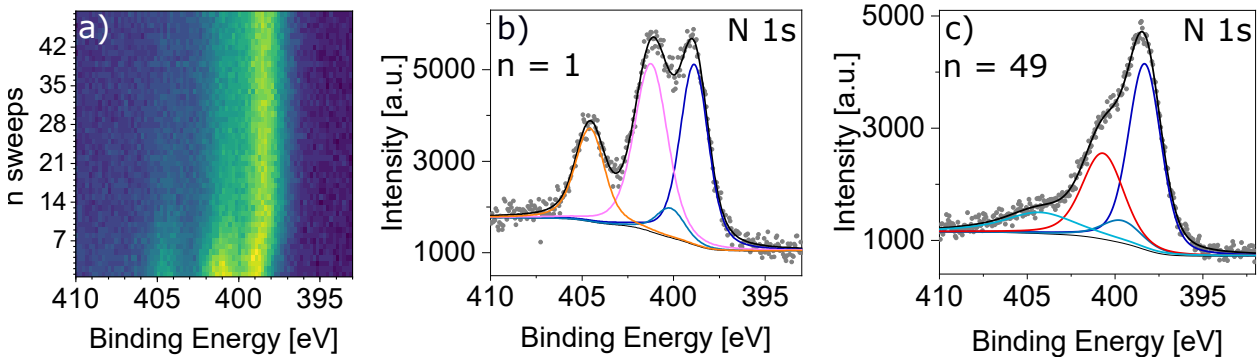

Figure S4: Series of N 1s XPS sweeps of a sub-ML TAH on HOPG (49 sweeps, time/sweep=3:49 min; n=1 after 8 min X-ray illumination, n=49 after 190 min). (a) The 2D plot of the sweeps indicates the azide loss, the transformation into amino or azo side groups and a concomitant shift in the heptazine nitrogen peaks that might be related to reordering on the support. (b) and (c) show detailed spectra for sweep n=1 and n=49 with peak fits by Voigt functions on a Shirley background. Binding energies, intensities and assignments are indicated in Table S1. While the first sweep can be described consistently as an azide layer with two azide and two heptazine nitrogen species (intensity ratio 3:6:1:6), the last sweep, n=49, consists in majority of a reacted heptazine layer with amino or azo side groups, while some intact azide groups are still present.

Table S1: N 1s XPS binding energies and relative peak intensities for the XPS data shown in Fig. S4b and c, with the color code that maps the respective fitted peaks. The obtained binding energies are altogether slightly shifted by about 0.6 eV with respect to those obtained on Au(111) (see Section S5), probably due to enhanced core hole shielding on the metal support. The π-excitation peak is relevant only for polymerized heptazine units. The ratio N (side) atoms per heptazine unit is calculated as ratio of the relative intensities (indicated by the colored bullets) and taking into account that the heptazine ring contains 7 N atoms. The indication of a range reflects exclusion, resp. inclusion of the π-excitation into the sum of heptazine relative peak intensities.

Peak	E_B [eV]		rel. intensity	
	n = 1	n = 49	n = 1	n = 49
● N (heptazine ring)	398.9	398.3	≡6	5.9
● N (heptazine core)	400.2	399.6	≡1	1.0
● N (π-excitation)	-	404.3	-	1.9
● N (azide - outer N's)	401.2	-	6.5	0
● N (azide - central N)	404.6	-	3.3	0
● N (side)	-	400.7	–	3.5
N (side) atoms (●) per heptazine unit (●●/●)	–	–	–	2.8 – 3.5

The XPS data allows us to estimate the average type of linking that results from the X-ray activation on HOPG. By comparing the obtained value of $\geq$ 2.8 N (side) atoms per heptazine unit with the values expected for different linking motifs in Table S2, we conclude that the obtained network contains more linking nitrogen atoms per heptazine unit than expected for a perfect 2D network formed by tertiary or secondary amine nodes. Note that the N (side) atom ratio is only indicative, since calculated from single sweeps.

Our values point rather to linear networks predominantly formed by azo groups or secondary amines, with a considerable presence of terminal amine groups that cannot be quantified separately. This is consistent with our observations in the STM images in Fig. S5: The loosely connected network, observed after short annealing to 676 K to remove residual azide groups and increase the surface order, is highly mobile and gets displaced by the scanning tip as seen in subsequent images.

Table S2: Number of N (side) atoms per heptazine unit for different types of linkers

Type of side group	Number N (side) per ring	Carbon nitride stoichiometry
Tertiary amine	1	C_3N_4
Secondary amine	1.5	$C_3N_{4.5}$
Primary (terminal) amine or azo group	3	C_3N_5

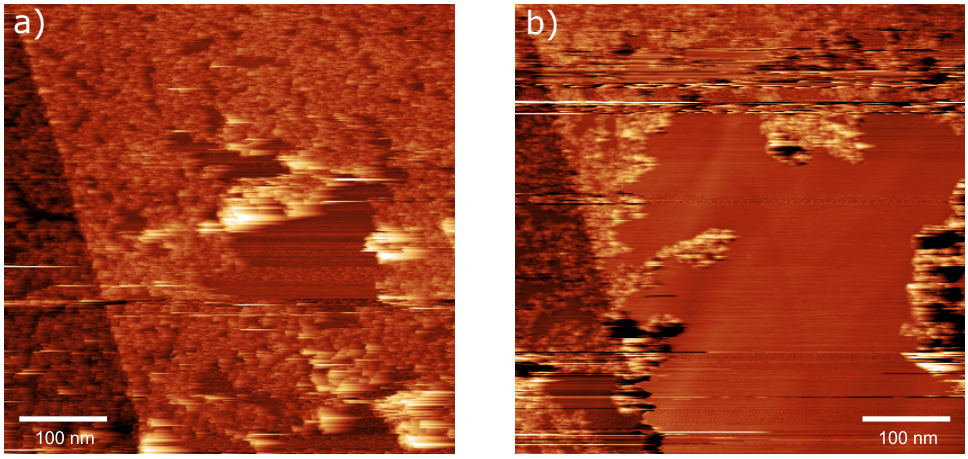

Figure S5: Two subsequent STM images of the heptazine network obtained by X-ray induced electron activation on HOPG and subsequent annealing to 676 K. The scanning tip continuously displaces the loosely connected molecule carpet, opening up large areas of the bare support especially where streaky, bright (strongly interacting) patches have been observed previously. *STM imaging parameters*: (a) $U_b = 3$ V, $I_t = 300$ pA, (b) $U_b = 2$ V, $I_t = 300$ pA.

S5. XPS analysis of the heptazine network on Au(111)

Table S3: XPS binding energies and relative peak intensities for the XPS data shown in the main text: a) after photochemical reaction of TAH with subsequent annealing (Fig. 2), b) after thermal reaction (Fig. 4). The color code maps the respective fitted peaks in the figures: Two nitrogen peaks fit the heptazine, one for the six ring atoms and one for the central tertiary amine atom, as well as a third broad peak that represents the π-excitation shake-up satellite related to the conjugated ring system. Linking or terminal amine or azo side groups appear all at similar binding energies and are represented by a single N (side) peak. This peak assignment and the relative binding energy values are in line with the compilation of experimental carbon nitride powder XPS spectra and their simulation by Zhang et al.,[5] although our observed binding energy values are lower by up to 1 eV, which might be related to the interaction with the support. The ratio N (side) atoms per heptazine unit is calculated as ratio of the relative intensities (indicated by the colored bullets) and taking into account that the heptazine ring contains 7 N atoms. The indication of a range reflects exclusion, resp. inclusion of the π-excitation into the sum of heptazine relative peak intensities. Contaminant peaks stemming from the deposition process are marked in grey: Adventitious carbon, also found for powder samples, as well as an unknown carbon species with very low, carbide-like binding energy, and an unknown nitrogen species with rather high binding energy that does not belong to amorphous carbon nitride.[6]

Peak	E_B [eV]	a) photo-+thermal reaction rel. intensity	b) thermal reaction rel. intensity
● N (heptazine ring)	397.9	≡6	≡6
● N (heptazine core)	399.2	≡1	≡1
● N (π-excitation)	403.4	1.6	1.0
● N (side)	400.4	2.5	2.3
● N (unknown)	402.3	1.1	–
N (side) atoms (●) per heptazine unit (●●/●)	–	2.0 – 2.5	2.0 – 2.3
● C (heptazine)	287.2	≡6	≡6
● C (adventitious carbon)	284.6	0.9	4.0
● C (unknown)	282.4	2.2	1.1

As the XPS analysis demonstrates, both preparation approaches lead to similar values of 2.0 – 2.3 and 2.0 – 2.5 N (side) atoms per heptazine unit, depending on whether or not the π-excitation is included. Comparing with the numbers expected for different linking motifs in Table S2, we can exclude that our networks are exclusively azo-linked. The irreversible

covalent bond formation upon polymerization favours rather amorphous and defect-rich networks with a high amount of terminal amines. Without their separate quantification, a clear attribution of the linking motifs remains elusive. The network is, however, more interconnected than on HOPG ($\geq$ 2.8 N (side) atoms per heptazine unit and high mobility in STM).

References

(1) Sattler, A. Investigations into s-Heptazine-Based Carbon Nitride Precursors. Ph.D. thesis, Ludwig-Maximilians-Universität (LMU), Munich, 2010.

(2) Saplinova, T.; Bakumov, V.; Gmeiner, T.; Wagler, J.; Schwarz, M.; Kroke, E. 2,5,8-Trihydrazino-s-heptazine: A precursor for heptazine-based iminophosphoranes. *Zeitschrift fur Anorganische und Allgemeine Chemie* **2009**, *635*, 2480–2487.

(3) Miller, D. R.; Swenson, D. C.; Gillan, E. G. Synthesis and structure of 2, 5, 8-triazido-s-heptazine: An energetic and luminescent precursor to nitrogen-rich carbon nitrides. *Journal of the American Chemical Society* **2004**, *126*, 5372–5373.

(4) Miller, D. R.; Holst, J. R.; Gillan, E. G. Nitrogen-rich carbon nitride network materials via the thermal decomposition of 2, 5, 8-triazido-s-heptazine. *Inorganic chemistry* **2007**, *46*, 2767–2774.

(5) Zhang, J. R.; Ma, Y.; Wang, S. Y.; Ding, J.; Gao, B.; Kan, E.; Hua, W. Accurate K-edge X-ray photoelectron and absorption spectra of g-C_3N_4 nanosheets by first-principles simulations and reinterpretations. *Physical Chemistry Chemical Physics* **2019**, *21*, 22819–22830.

(6) Titantah, J.; Lamoen, D. Carbon and nitrogen 1s energy levels in amorphous carbon nitride systems: XPS interpretation using first-principles. *Diamond and related materials* **2007**, *16*, 581–588.